Utilizing Symmetry Coupling Schemes in *Ab Initio* Nuclear Structure Calculations

T. Dytrych[a], J. P. Draayer[a], K. D. Launey[a], P. Maris[b], J. P. Vary[b] and D. Langr[c]

[a] *Department of Physics and Astronomy, Louisiana State University, Baton Rouge, LA 70803, USA*
[b] *Department of Physics and Astronomy, Iowa State University, Ames, IA 50011, USA*
[c] *Department of Computer Systems, Czech Technical University, Prague, Czech Republic*

Abstract

We report on *ab initio* no-core shell model calculations in a symmetry-adapted SU(3)-based coupling scheme that demonstrate that collective modes in p-shell nuclei emerge from first principles. The low-lying states of ^{6}Li, ^{6}He, ^{8}Be, ^{8}B, ^{12}C, and ^{16}O, are shown to exhibit orderly patterns that favor spatial configurations with strong quadrupole deformation and complementary low intrinsic spin values, a picture that is consistent with the nuclear symplectic model. The results also suggest a pragmatic path forward to accommodate deformation-driven collective features in *ab initio* analyses when they dominate the nuclear landscape.

Keywords: *No-core shell model; SU(3) coupling scheme; p-shell nuclei*

1 Introduction

In the last few years, *ab initio* approaches to nuclear structure and reactions have considerably advanced our understanding and capability of achieving first-principle descriptions of p-shell nuclei [1–3]. These advances are driven by the major progress in the development of realistic nuclear potential models, such as J-matrix inverse scattering potentials [4] and two- and three-nucleon potentials derived from meson exchange theory [5] or by using chiral effective field theory [6], and, at the same time, by the utilization of massively parallel computing resources [7–9].

The predictive power that *ab initio* models hold [10, 11] makes them suitable for targeting short-lived nuclei that are inaccessible by experiment but essential to further modeling, for example, of the dynamics of X-ray bursts and the path of nucleosynthesis (see, e. g., Refs. [12, 13]). The main limitation of *ab initio* approaches is inherently coupled with the combinatorial growth in the size of the many-particle model space with increasing nucleon numbers and expansion in the number of single-particle levels in the model space as illustrated in Fig. 1. This points to the need of further major advances in many-body methods to access a wider range of nuclei and experimental observables, while retaining the *ab initio* predictive power.

These considerations motivate us to develop and investigate a novel model, the *ab initio* symmetry-adapted no-core shell model (SA-NCSM) [14], which by taking advantage of symmetries inherent to the nuclear dynamics [15, 16] allows one to truncate a model space according to correlations indispensable for modeling important modes of nuclear collective dynamics, thereby overcoming the scale explosion bottleneck of *ab initio* nuclear structure computations.

Proceedings of International Conference 'Nuclear Theory in the Supercomputing Era — 2013' (NTSE-2013), Ames, IA, USA, May 13–17, 2013. Eds. A. M. Shirokov and A. I. Mazur. Pacific National University, Khabarovsk, Russia, 2014, p. 62.
http://www.ntse-2013.khb.ru/Proc/Dytrych.pdf.

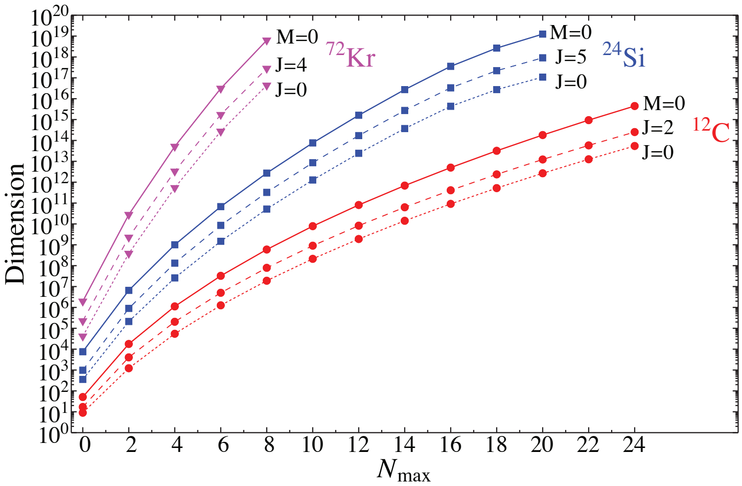

Figure 1: The dimensions of positive parity model spaces as functions of $N_{\max}$ for selected nuclei. Solid curves show the number of basis states with the projection of the total angular momentum $M = 0$. Dashed and dotted curves depict the number of basis states carrying selected values of the total angular momentum J.

2 *Ab initio* calculations in a SU(3)-based coupling scheme

The SA-NCSM joins a no-core shell model (NCSM) theory [2] with a multi-shell, SU(3)-based coupling scheme [15, 17]. Specifically, the many-nucleon basis states of the SA-NCSM are decomposed into spatial and intrinsic spin parts, where the spatial part is further classified according to the SU(3) $\supset$ SO(3) group chain. The significance of the SU(3) group for a microscopic description of the nuclear collective dynamics can be seen from the fact that it is the symmetry group of the successful Elliott model [15], and a subgroup of the physically relevant Sp$(3,\mathbb{R})$ symplectic model [16], which provides a comprehensive theoretical foundation for understanding the dominant symmetries of nuclear collective motion. The SA-NCSM basis states are labeled as

$$|\vec{\gamma}; N(\lambda\,\mu)\kappa L; (S_p S_n)S; JM\rangle, \tag{1}$$

where N signifies the number of harmonic oscillator quanta with respect to the minimal number for a given nucleus. Quantum numbers S_p, S_n, and S denote proton, neutron, and total intrinsic spins, respectively, and $(\lambda\,\mu)$ represent a set of quantum numbers associated with SU(3) irreducible representations, irreps. The label κ distinguishes multiple occurrences of the same orbital momentum L in the parent irrep $(\lambda\,\mu)$. The L is coupled with S to the total angular momentum J and its projection M. The basis states bring forward important information about nuclear shapes and deformation according to an established mapping [18]. For example, (00), $(\lambda\,0)$ and $(0\,\mu)$ describe spherical, prolate and oblate shapes, respectively. The symbol $\vec{\gamma}$ schematically denotes the additional quantum numbers needed to specify a distribution of nucleon clusters over the major HO shells and their inter-shell coupling. Specifically, in each major HO shell η with degeneracy Ω_η, clusters of protons and neutrons are arranged into antisymmetric $\mathrm{U}(\Omega_\eta) \times \mathrm{SU}(2)_{S_\eta}$ irreps [19], with $\mathrm{U}(\Omega_\eta)$ further reduced with respect to SU(3). The quantum numbers, $\left[f_1, \ldots, f_{\Omega_\eta}\right] \alpha_\eta \left(\lambda_\eta\, \mu_\eta\right) S_\eta$, along with $\mathrm{SU}(3) \times \mathrm{SU}(2)_S$ labels of inter-shell coupling unambiguously determine SA-NCSM basis states (1). Note that a spatial symmetry associated with a Young shape $[f_1, \ldots, f_{\Omega_\eta}]$ is uniquely determined by the imposed antisymmetrization and the associated intrinsic spin S_η. A multiplicity index α_η is required to distinguish multiple occurrences of SU(3) irrep $(\lambda_\eta\,\mu_\eta)$ in a given U(Ω_η) irrep. It is important to note that any model space spanned by a complete set of equivalent SU(3) $\times$ SU(2)$_S$ irreps, that is, a space spanned by all configurations carrying a fixed set of $S_p\,S_n\,S$ and $(\lambda\,\mu)$ quantum numbers, permits exact factorization of the center-of-mass motion.

The SA-NCSM implements fast methods for calculating matrix elements of arbitrary (currently up to two-body, but expandable to higher-rank) operators in the symmetry-adapted basis. This facilitates both the evaluation of the Hamiltonian matrix elements and the use of the resulting eigenvectors to evaluate other experimental observables. The underlying principle behind the SA-NCSM computational kernel is an SU(3)-type Wigner–Eckhart theorem, which factorizes interaction matrix elements into the product of SU(3) reduced matrix elements (*rme*) and the associated SU(3) coupling coefficient. The SA-NCSM configurations are constructed by the inter-shell coupling of a sequence of single-shell nucleon clusters arranged into U(Ω) $\times$ SU(2)$_S$, with U(Ω) $\supset$ SU(3), irreps. Therefore, all the multi-shell *rme* are constructed from a set of single-shell *rme* computed in a configuration space of these irreps. This reduces the number of key pieces of information required to the single-shell *rme*, and these track with the number of U(Ω) $\times$ SU(2)$_S$ irreps, with U(Ω) $\supset$ SU(3), that represent building blocks of the SA-NCSM approach. It is therefore significant that their number grows slowly with the increasing nucleon number and $N_{\max}$ cutoff as this allows these key pieces of information to be stored in CPU memory.

3 Structure of nuclear wave functions

The expansion of calculated eigenstates in the physically relevant SU(3) basis unveils salient features that emerge from the complex dynamics of these strongly interacting many-particle systems. To explore the nature of the most important correlations, we analyze the probability distribution across Pauli-allowed $(S_p\,S_n\,S)$ and $(\lambda\,\mu)$ configurations of the four lowest-lying isospin-zero ($T=0$) states of ^{6}Li ($1^+_{\rm gs}$, 3^+_1, 2^+_1, and 1^+_2), the ground-state rotational bands of ^{8}Be, ^{6}He and ^{12}C, the lowest 1^+, 3^+, and 0^+ excited states of ^{8}B, and the ground state of ^{16}O. Results for the ground state of ^{6}Li and ^{8}Be, obtained with the JISP16 and chiral N^{3}LO interactions, respectively, are shown in Figs. 2 and 3. These figures illustrates a feature common to all the low-energy solutions considered; namely, a highly structured and regular mix of intrinsic spins and SU(3) spatial quantum numbers that has heretofore gone unrecognized in other *ab initio* studies, and which, furthermore, does not seem to depend on the particular choice of realistic NN potential.

For a closer look at these results, first consider the spin content. We found that the calculated eigenstates project at a 99% level onto a comparatively small subset of intrinsic spin combinations. For instance, the lowest-lying eigenstates in ^{6}Li are almost entirely realized in terms of configurations characterized by the following intrinsic spin $(S_p\,S_n\,S)$ triplets: $\left(\frac{3}{2}\,\frac{3}{2}\,3\right)$, $\left(\frac{1}{2}\,\frac{3}{2}\,2\right)$, $\left(\frac{3}{2}\,\frac{1}{2}\,2\right)$, and $\left(\frac{1}{2}\,\frac{1}{2}\,1\right)$, with the last one carrying over 90% of each eigenstate. Likewise, the same spin components as in the case of ^{6}Li are found to dominate the ground state and the lowest 1^+, 3^+, and 0^+ excited states of ^{8}B (Table 1). The ground state bands of ^{8}Be, ^{6}He, ^{12}C, and ^{16}O are found to be dominated by many-particle configurations carrying total intrinsic spin of the protons and neutrons equal to zero and one, with the largest contributions due to $(S_p\,S_n\,S) = (0\,0\,0)$ and $(1\,1\,2)$ configurations.

Second, consider the spatial degrees of freedom. Our results show that the mixing of $(\lambda\,\mu)$ quantum numbers, induced by the SU(3) symmetry breaking terms of realistic interactions, exhibits a remarkably simple pattern. One of its key features is the preponderance of a single $0\hbar\Omega$ SU(3) irrep. This so-called leading irrep, according to the established geometrical interpretation of SU(3) labels $(\lambda\,\mu)$ [18], is characterized

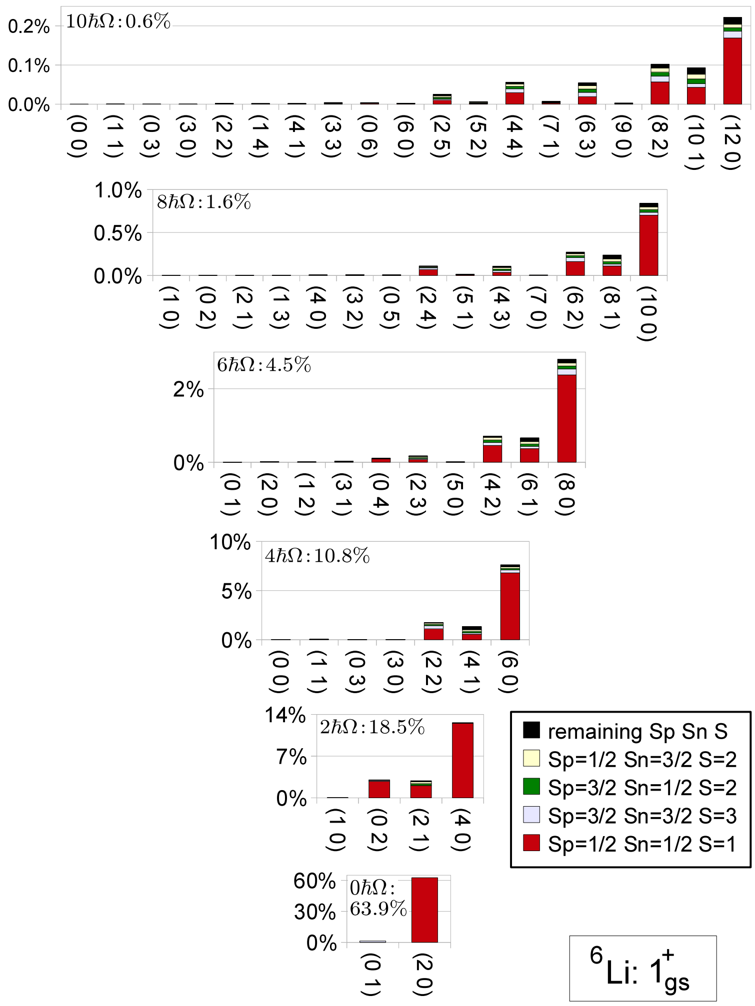

Figure 2: Probability distributions for proton, neutron, and total intrinsic spin components $(S_p\, S_n\, S)$ across the Pauli-allowed $(\lambda\, \mu)$ values (horizontal axis) for the calculated 1^+ ground state of ^{6}Li obtained for $N_{\max} = 10$ and $\hbar\Omega = 20$ MeV with the JISP16 interaction. The total probability for each $N\hbar\Omega$ subspace is given in the upper left-hand corner of each histogram. Adapted from Ref. [14].

by the largest value of the intrinsic quadrupole deformation. For instance, the low-lying states of ^{6}Li project at a 40%–70% level onto the prolate $0\hbar\Omega$ SU(3) irrep $(2\,0)$, as illustrated in Figs. 2 and 3 for the ground state. For the considered states of

Table 1: Probability amplitude of the dominant $(S_p\, S_n\, S)$ spin configuration and the dominant nuclear shapes according to Eq. (2) for the ground state of p-shell nuclei.

Nucleus	$(S_p\, S_n\, S)$	Prob. [%]	$(\lambda_0\, \mu_0)$	Prob. [%]
^{6}Li	$(\frac{1}{2}\,\frac{1}{2}\,1)$	93.26	$(2\,0)$	98.13
^{8}B	$(\frac{1}{2}\,\frac{1}{2}\,1)$	85.17	$(2\,1)$	87.94
^{8}Be	$(0\,0\,0)$	85.25	$(4\,0)$	90.03
^{12}C	$(0\,0\,0)$	55.19	$(0\,4)$	48.44
^{16}O	$(0\,0\,0)$	83.60	$(0\,0)$	89.51

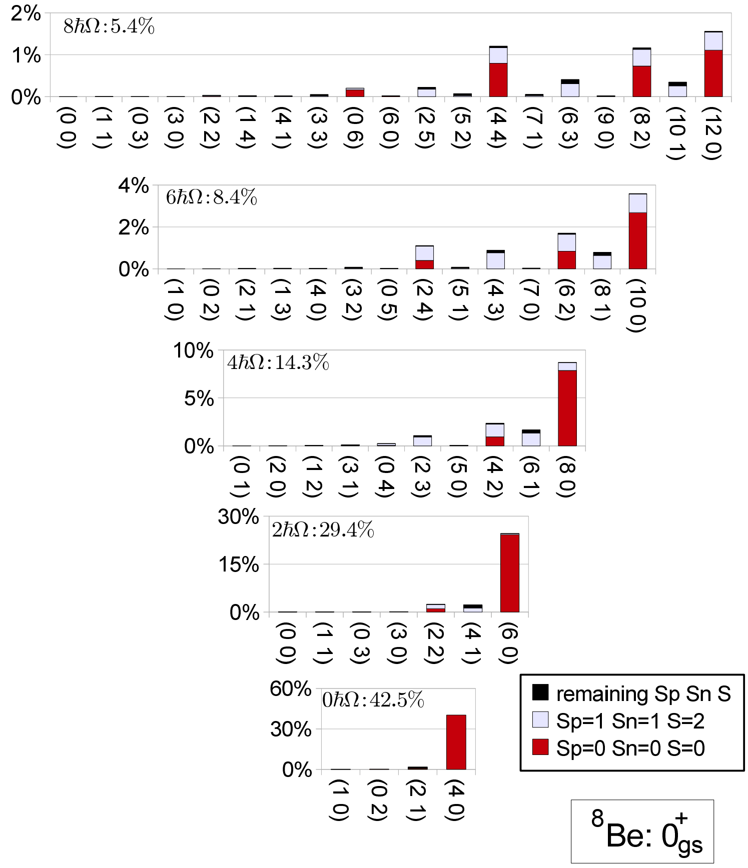

Figure 3: Probability distributions for proton, neutron, and total intrinsic spin components ($S_p\, S_n\, S$) across the Pauli-allowed ($\lambda\, \mu$) values (horizontal axis) for the calculated 0^+ ground state of ^{8}Be obtained for $N_{\max} = 8$ and $\hbar\Omega = 25$ MeV with the chiral N^{3}LO interaction. The total probability for each $N\hbar\Omega$ subspace is given in the upper left-hand corner of each histogram. Adapted from Ref. [14].

^{8}B, ^{8}Be, ^{12}C, and ^{16}O, qualitatively similar dominance of the leading $0\hbar\Omega$ SU(3) irreps is observed — (2 1), (4 0), (0 4), and (0 0) irreps, associated with triaxial, prolate, oblate, and spherical shapes, respectively. The clear dominance of the most deformed $0\hbar\Omega$ configuration within low-lying states of light p-shell nuclei indicates that the quadrupole-quadrupole interaction of the Elliott SU(3) model of nuclear rotations [15] is realized naturally within an *ab initio* framework.

The analysis also reveals that the dominant SU(3) basis states at each $N\hbar\Omega$ subspace ($N = 0, 2, 4, \ldots$) are typically those with ($\lambda\, \mu$) quantum numbers given by

$$\lambda + 2\mu = \lambda_0 + 2\mu_0 + N \tag{2}$$

where λ_0 and μ_0 denote labels of the leading SU(3) irrep in the $0\hbar\Omega$ ($N = 0$) subspace. We conjecture that this regular pattern of SU(3) quantum numbers reflects the presence of an underlying symplectic Sp(3, $\mathbb{R}$) symmetry of microscopic nuclear collective motion [16] that governs the low-energy structure of both even-even and odd-odd p-shell nuclei. This can be seen from the fact that ($\lambda\, \mu$) configurations that satisfy condition (2) can be determined from the leading SU(3) irrep ($\lambda_0\, \mu_0$) through a successive application of a specific subset of the Sp(3, $\mathbb{R}$) symplectic $2\hbar\Omega$ raising operators. This subset is composed of the three operators, $\hat{A}_{zz}$, $\hat{A}_{zx}$, and $\hat{A}_{xx}$, that distribute two oscillator quanta in z and x directions, but none in y direction, thereby inducing

SU(3) configurations with ever-increasing intrinsic quadrupole deformation. These three operators are the generators of the $\mathrm{Sp}(2,\mathbb{R}) \subset \mathrm{Sp}(3,\mathbb{R})$ subgroup [20], and give rise to deformed shapes that are energetically favored by an attractive quadrupole-quadrupole interaction [21]. Note that this is consistent with our earlier findings of a clear symplectic $\mathrm{Sp}(3,\mathbb{R})$ structure with the same pattern (2) in *ab initio* eigensolutions for ^{12}C and ^{16}O [22].

Furthermore, there is an apparent hierarchy among states that fulfill condition (2). In particular, the $N\hbar\Omega$ configurations with $(\lambda_0{+}N\ \mu_0)$, the so-called stretched states, carry a noticeably higher probability than the others. For instance, the $(2+N\ 0)$ stretched states contribute at the 85% level to the ground state of ^{6}Li, as can be readily seen in Figs. 2 and 3. Moreover, the dominance of the stretched states is rapidly increasing with the increasing many-body basis cutoff $N_{\max}$ as illustrated in Fig. 4. The sequence of the stretched states is formed by consecutive applications of the $\hat{A}_{zz}$ operator, the generator of $\mathrm{Sp}(1,\mathbb{R}) \subset \mathrm{Sp}(2,\mathbb{R}) \subset \mathrm{Sp}(3,\mathbb{R})$ subgroup, over the leading SU(3) irrep. This translates into distributing N oscillator quanta along the direction of the z-axis only and hence rendering the largest possible deformation. The important role of the stretched configurations for the description of the rotational bands in $N = Z$ even-even nuclei was recognized heretofore using a simple microscopic Hamiltonian [23]. In the present study, for the first time, this structure is clearly and simply unveiled within the context of a fully microscopic framework starting from first principles.

4 Efficacy of the SU(3) basis

The observed patterns of intrinsic spin and deformation mixing supports a symmetry-guided basis selection philosophy referenced above. Specifically, one can take advantage of dominant symmetries to refine the definition of the NCSM model space, which is based solely on the $N_{\max}$ cutoff. A SA-NCSM model space, which we denote as $\langle N^{\perp}_{\max}\rangle N^{\top}_{\max}$, can be constructed using a symmetry-guided selection that includes the complete basis up through some $N^{\perp}_{\max} \leq N_{\max}$ along with configurations carrying a restricted set of $(\lambda\,\mu)$ and $(S_p\,S_n\,S)$ quantum numbers in the $N^{\perp}_{\max}$ to $N^{\top}_{\max}$ space. Ultimately, we aim to achieve $N^{\top}_{\max} \geq N_{\max}$, where $N_{\max}$ is the largest value for which complete-space results can be currently calculated. This concept focuses on retaining the most important configurations that support the strong many-nucleon correlations of a nuclear system using the underlying $\mathrm{Sp}(1,\mathbb{R}) \subset \mathrm{Sp}(2,\mathbb{R}) \subset \mathrm{Sp}(3,\mathbb{R})$ symmetry considerations. Within this context, it is important to note that for model spaces truncated according to $(\lambda\,\mu)$ irreps and intrinsic spins $(S_p\,S_n\,S)$, the spurious center-of-mass motion can be factored out exactly, which represents an important advantage of this scheme.

The efficacy of the symmetry-guided concept is illustrated for SA-NCSM results obtained in a model space, which is expanded beyond the complete $N^{\perp}_{\max} = 6$ (or 8) space by relatively few dominant intrinsic spin components and quadrupole deformations that satisfy condition (2). We use selected spaces up through $N^{\top}_{\max} = 12$, which allows a comparison to available results obtained in the complete $N_{\max} = 12$ space and hence, probes the efficacy of the SA-NCSM symmetry-guided model space selection concept. For this analysis, a Coulomb plus bare JISP16 NN interaction for $\hbar\Omega$ values ranging from 17.5 up to 25 MeV is used. SA-NCSM eigenstates are used to determine spectroscopic properties of low-lying $T = 0$ states of ^{6}Li for a $\langle 6\rangle 12$ model space and of the ground-state band of ^{6}He for $\langle 8\rangle 12$. We utilize a complete space of $N^{\perp}_{\max} = 6$ for ^{6}Li and of $N^{\perp}_{\max} = 8$ for ^{6}He, as these spaces seem sufficient to accommodate essential mixing of low-energy HO excitations.

The results indicate that the observables obtained in the symmetry-guided truncated spaces under consideration are excellent approximations to the corresponding complete-space counterparts. In particular, the ground-state binding energies repre-

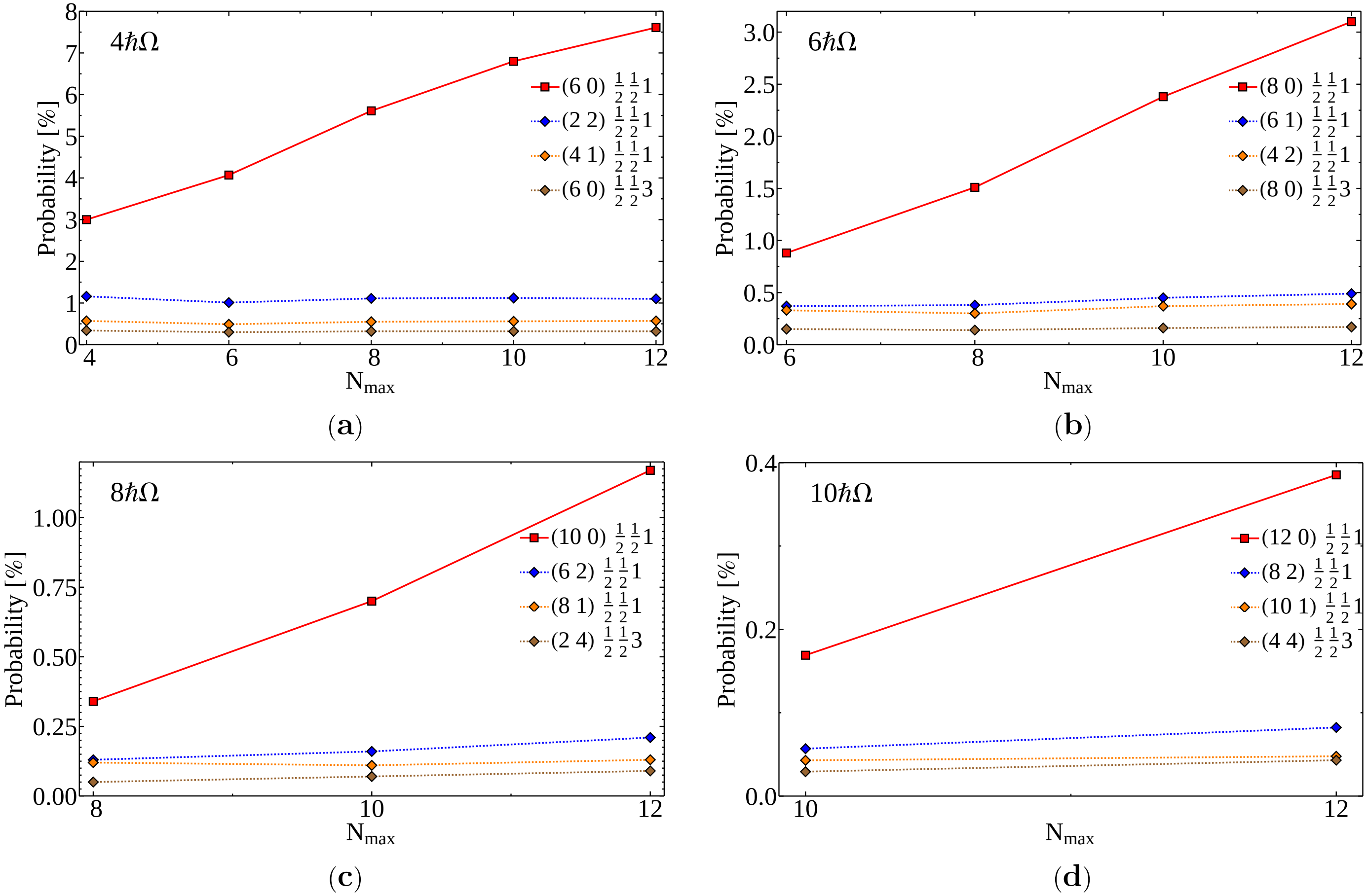

Figure 4: Probabilities of the most important $(\lambda\,\mu)$ $(S_p\,S_n\,S)$ components in ^{6}Li at $4\hbar\Omega$ subspace (a), $6\hbar\Omega$ subspace (b), $8\hbar\Omega$ subspace (c), and $10\hbar\Omega$ subspace as a function of the model space cutoff $N_{\max}$.

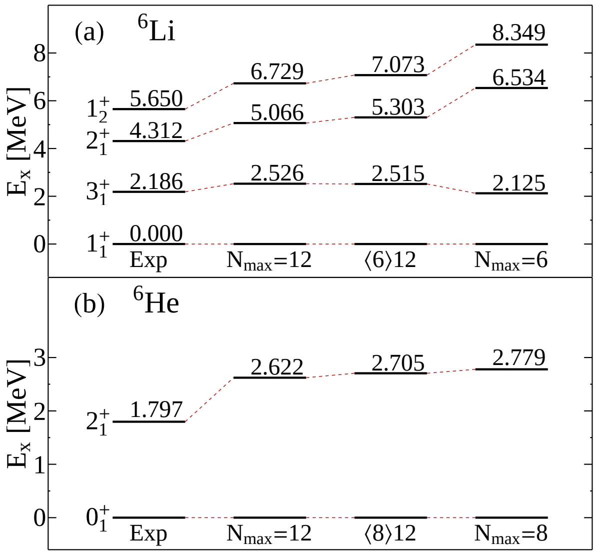

Figure 5: Experimental and theoretical excitation energies: (a) $T = 0$ states of ^{6}Li, and (b) the two lowest-lying states of the halo ^{6}He nucleus. Experimental results [24] are given in the first column. The theoretical results shown are for JISP16 and $\hbar\Omega = 20$ MeV in the complete $N_{\max} = 12$ space (second column), symmetry-guided truncated model space (third column) and the complete $N_{\max} = 6$ or 8 spaces (last column). Note the relatively large change in the calculated excitation spectrum of ^{6}Li when $N_{\max}$ is increased from 6 to 12, and that the $\langle 6\rangle 12$ SA-NCSM results (third column) track the latter closely.

sent from 98% up to 98.7% of the complete-space binding energy in the case of ^{6}Li, and reach over 99% for ^{6}He. Furthermore, the excitation energies differ only by 11 keV to a few hundred keV from the corresponding complete-space results, see Fig. 5, and the agreement with known experimental data is reasonable over a broad range of $\hbar\Omega$ values.

As illustrated in Table 2, the magnetic dipole moments for ^{6}Li agree to within 0.3% for odd-J values, and 5% for $\mu(2^+_1)$. Qualitatively similar agreement is achieved for $\mu(2^+_1)$ of ^{6}He, as shown in Table 3. The results suggest that it may suffice to include all low-lying $\hbar\Omega$ states up to a fixed limit, e. g., $N^{\perp}_{\max} = 6$ for ^{6}Li and $N^{\perp}_{\max} = 8$ for ^{6}He, to account for the most important correlations that contribute to the magnetic dipole moment.

To explore how close one comes to reproducing the important long-range correlations of the complete $N_{\max} = 12$ space in terms of nuclear collective excitations within

Table 2: Magnetic dipole moments μ [μ_N] and point-particle rms matter radii r_m [fm] of $T = 0$ states of ^{6}Li calculated in the complete $N_{\max} = 12$ space and the $\langle 6\rangle 12$ subspace for JISP16 and $\hbar\Omega = 20$ MeV. The experimental value for the 1^+ ground state is known to be $\mu = +0.822\ \mu_N$ [24].

	$1^+_1 0$	$3^+_1 0$	$2^+_1 0$	$1^+_2 0$
μ				
Full $N_{\max} = 12$	0.838	1.866	0.960	0.336
$\langle 6\rangle 12$	0.840	1.866	1.015	0.337
rms				
Full $N_{\max} = 12$	2.146	2.092	2.257	2.373
$\langle 6\rangle 12$	2.139	2.079	2.236	2.355

Table 3: Selected observables for the two lowest-lying states of ^{6}He obtained in the complete $N_{\max} = 12$ space and $\langle 8\rangle 12$ model subspace for JISP16 and $\hbar\Omega = 20$ MeV.

	$N_{\max} = 12$	$\langle 8\rangle 12$
$B(E2; 2_1^+ \to 0_1^+)$ [e^2fm^4]	0.181	0.184
$Q(2_1^+)$ [e·fm^2]	−0.690	−0.711
$\mu(2_1^+)$ [μ_N]	−0.873	−0.817
r_m (2_1^+) [fm]	2.153	2.141
r_m (0_1^+) [fm]	2.113	2.110

the symmetry-truncated spaces under consideration, we compared observables that are sensitive to the tails of the wavefunctions; specifically, the point-particle rms matter radii, the electric quadrupole moments and the reduced electromagnetic $B(E2)$ transition strengths that, in addition, could hint at rotational features [25]. As Table 3 clearly shows, the complete-space results for these observables are remarkably well reproduced by the SA-NCSM for ^{6}He in the restricted $\langle 8\rangle 12$ space. Similarly, the $\langle 6\rangle 12$ eigensolutions for ^{6}Li yield results for $B(E2)$ strengths and quadrupole moments that track very closely with their complete $N_{\max} = 12$ space counterparts for all values of $\hbar\Omega$ (Fig. 6). The $B(E2)$ strengths almost double upon increasing the model space from $N_{\max} = 6$ to $N_{\max} = 12$. This result suggests that further expansion of the model space will be needed to reach convergence [26]. The close correlation between the $N_{\max} = 12$ and $\langle 6\rangle 12$ results is nevertheless impressive. In addition to being in agreement, the results reproduce the challenging sign and magnitude of the ground-state quadrupole moment that is measured to be $Q(1^+) = -0.0818(17)$ e·fm^2 [24].

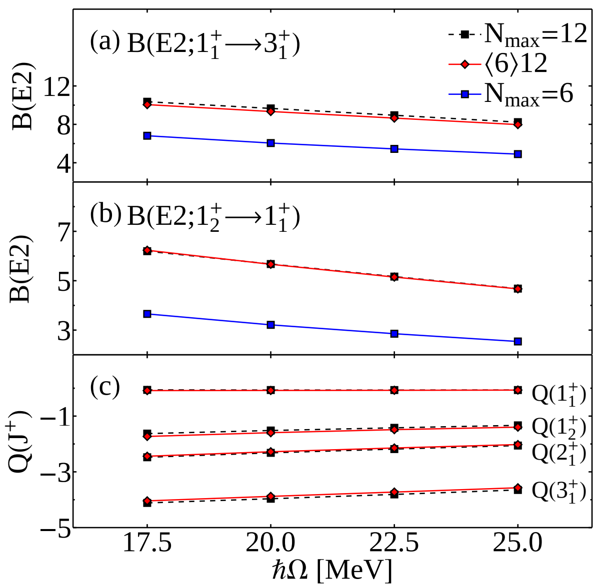

Figure 6: Electric quadrupole transition probabilities in units of e^2fm^4 [(a) and (b), as shown], and quadrupole moments in units of e·fm^2 (c) as a function of $\hbar\Omega$ for $T = 0$ states of ^{6}Li calculated using JISP16 in the complete $N_{\max} = 12$ space (dashed black line), the complete $N_{\max} = 6$ space (solid blue line), and symmetry-truncated $\langle 6\rangle 12$ (solid red line) model spaces. Note that while the $N_{\max} = 6$ results differ considerably from their $N_{\max} = 12$ counterparts, in all cases the latter are nearly indistinguishable from the truncated $\langle 6\rangle 12$ results. Experimentally, $B(E2; 1_1^+ \to 3_1^+) = 25.6(20)$ e^2fm^4 [24].

Finally, the results for the rms matter radii of ^{6}Li, listed in Table 2, agree to within 1%.

The differences between truncated-space and complete-space results are found to be essentially insensitive to the choice of $\hbar\Omega$ and appear sufficiently small as to be inconsequential relative to the residual dependences on $\hbar\Omega$ and on $N_{\max}$ (see Fig. 6). Since the NN interaction dominates contributions from three-nucleon forces (3NFs) in light nuclei, except for selected cases [27–29], we expect our results to be robust and carry forward to planned applications that will include 3NFs.

5 Conclusion

We have developed a novel approach that capitalizes on advances being made in *ab initio* methods while exploiting exact and partial symmetries of nuclear many-body system. Using this approach we have demonstrated that the low-lying eigenstates of ^{6}Li, ^{8}Be, ^{12}C, and ^{16}O, which were obtained using the JISP16 and N^{3}LO NN interaction, exhibit a strong dominance of few intrinsic spin components and carry an intriguingly simple pattern of dominant deformations. The results very clearly underscore the significance of the SU(3) scheme, LS-coupling, and underlying symplectic symmetry in enabling an extension, through symmetry-guided model space reductions, of *ab initio* methods to heavier nuclei beyond ^{16}O.

Acknowledgments

This work was supported in part by the US NSF (OCI-0904874, OCI-0904782, PHY-0904782), the US Department of Energy (DE-SC0005248, DE-SC0008485, DE-FG02-87ER40371), and the Southeastern Universities Research Association. This research used computing resources of the Louisiana Optical Network Initiative, LSU's Center for Computation & Technology, and the National Energy Research Scientific Computing Center, which is supported by the Office of Science of the US Department of Energy under Contract No. DE-AC02-05CH11231.

References

[1] S. C. Pieper, R. B. Wiringa and J. Carlson, Phys. Rev. C **70**, 054325 (2004); K. M. Nollett, S. C. Pieper, R. B. Wiringa, J. Carlson and G. M. Hale, Phys. Rev. Lett. **99**, 022502 (2007).

[2] P. Navrátil, J. P. Vary and B. R. Barrett, Phys. Rev. Lett. **84**, 5728 (2000); Phys. Rev. C **62**, 054311 (2000); S. Quaglioni and P. Navrátil, Phys. Rev. Lett. **101**, 092501 (2008); Phys. Rev. C **79**, 044606 (2009); B. R. Barrett, P. Navrátil and J. P. Vary, Progr. Part. Nucl. Phys. **69**, 131 (2013).

[3] G. Hagen, T. Papenbrock and M. Hjorth-Jensen, Phys. Rev. Lett. **104**, 182501 (2010).

[4] A. M. Shirokov, A. I. Mazur, S. A. Zaytsev, J. P. Vary and T. A. Weber, Phys. Rev. C **70**, 044005 (2004); A. M. Shirokov, J. P. Vary, A. I. Mazur, S. A. Zaytsev and T. A. Weber, Phys. Lett. B **621**, 96(2005); A. M. Shirokov, J. P. Vary, A. I. Mazur and T. A. Weber, Phys. Lett. B **644**, 33 (2007).

[5] R. Machleidt, F. Sammarruca and Y. Song, Phys. Rev. C **53**, R1483 (1996); R. Machleidt, Phys. Rev. C **63**, 024001 (2001).

[6] D. R. Entem and R. Machleidt, Phys. Rev. C **68**, 041001 (2003).

[7] P. Sternberg, E. G. Ng, C. Yang, P. Maris, J. P. Vary, M. Sosonkina and H. V. Le, in *Proc. 2008 ACM/IEEE Conf. on Supercomputing, Austin, November 2008.* IEEE Press, Piscataway, NJ, 2008, p. 15:1.

[8] P. Maris, M. Sosonkina, J. P. Vary, E. G. Ng and C. Yang, Proc. Comput. Sci. **1**, 97 (2010).

[9] H. M. Aktulga, C. Yang, E. N. Ng, P. Maris and J. P. Vary, in *Euro-Par*, eds. C. Kaklamanis, T. S. Papatheodorou and P. G. Spirakis. Lecture Notes Comput. Sci. **7484**, 830 (2012).

[10] P. Maris, A. M. Shirokov and J. P. Vary, Phys. Rev. C **81**, 021301(R) (2010).

[11] V. Z. Goldberg *et al.*, Phys. Lett. B **692**, 307 (2010).

[12] B. Davids, R. H. Cyburt, J. Jose and S. Mythili, Astrophys. J. **735**, 40 (2011).

[13] A. M. Laird *et al.*, Phys. Rev. Lett. **110**, 032502 (2013).

[14] T. Dytrych, K. D. Launey, J. P. Draayer, P. Maris, J. P. Vary, E. Saule, U. Catalyurek, M. Sosonkina, D. Langr and M. A. Caprio, Phys. Rev. Lett., *in press*, arXiv:1312.0969 [nucl-th] (2013).

[15] J. P. Elliott, Proc. Roy. Soc. A **245**, 128 (1958); *ibid.* **245**, 562 (1958); J. P. Elliott and M. Harvey, *ibid.* **272**, 557 (1962).

[16] G. Rosensteel and D. J. Rowe, Phys. Rev. Lett. **38**, 10 (1977).

[17] J. P. Draayer, T. Dytrych, K. D. Launey and D. Langr, Progr. Part. Nucl. Phys. **67**, 516 (2012).

[18] O. Castaños, J. P. Draayer and Y. Leschber, Z. Phys. A **329**, 33 (1988); G. Rosensteel and D. J. Rowe, Ann. Phys. (NY) **104**, 134 (1977); Y. Leschber and J. P. Draayer, Phys. Lett. B **190**, 1 (1987).

[19] J. P. Draayer, Y. Leschber, S. C. Park and R. Lopez, Comput. Phys. Comm. **56**, 279 (1989).

[20] D. R. Peterson and K.T. Hecht, Nucl. Phys. A **344**, 361 (1980).

[21] D. J. Rowe, Rep. Progr. Phys. **48**, 1419 (1985).

[22] T. Dytrych, K. D. Sviratcheva, C. Bahri, J. P. Draayer and J. P. Vary, Phys. Rev. Lett. **98**, 162503 (2007).

[23] F. Arickx, Nucl. Phys. A **268**, 347 (1976).

[24] D. R. Tilley *et al.*, Nucl. Phys. A **708**, 3 (2002).

[25] M. A. Caprio, P. Maris and J. P. Vary, Phys. Lett. B **719**, 179 (2013).

[26] C. Cockrell, J. P. Vary and P. Maris, Phys. Rev. C **86**, 034325 (2012).

[27] B. R. Barrett, P. Navrátil and J. P. Vary, Progr. Part. Nucl. Phys. **69**, 131 (2013).

[28] P. Maris, J. P. Vary, P. Navrátil, W. E. Ormand, H. Nam and D. J. Dean, Phys. Rev. Lett. **106**, 202502 (2011).

[29] P. Maris, J. P. Vary and P. Navrátil, Phys. Rev. C **87**, 014327 (2013).